LIMNOLOGY
and
OCEANOGRAPHY: METHODS

Limnol. Oceanogr.: Methods 5, 2007, 396–406

LISST-100 measurements of phytoplankton size distribution: evaluation of the effects of cell shape

Lee Karp-Boss, Laura Azevedo, and Emmanuel Boss
School of Marine Sciences, University of Maine, Orono, Maine, USA

Abstract

Information on cell size is central to studies of phytoplankton ecology, yet in situ measurements of particle size distribution remain a challenge. The LISST-100 (Laser In Situ Scattering and Transmissometry; Sequoia Scientific, Inc.) is one of few commercially available instruments that provide autonomous measurements of size distributions of suspended particles in situ. Its capability to size phytoplankton needs to be evaluated, however, for two reasons. First, size is not measured directly; rather, information on size is obtained from near-forward scattering measurements that are inverted to obtain size distributions. The inversion assumes that particles are homogeneous spheres. Phytoplankton, however, display a wide range of cell shapes and their scattering behavior is likely to be different from that of spheres. Second, the LISST-100 was originally designed for sediments and its inversion assumes an index of refraction typical of inorganic particles. We compared size and volume concentration distributions obtained by the LISST-100 to those derived via microscopy for phytoplankton cultures of different cell sizes and shapes. Results demonstrate the success of the LISST-100 in measuring size and volume concentrations of cells with a cell aspect ratio that is close to 1 and illustrate its limitations when nonspherical cells are present in the sample. Uses of the LISST-100 in laboratory and field studies are discussed in light of the results from this study.

Cell size plays a fundamental regulatory role in phytoplankton community dynamics. Basic cell functions such as light and nutrient acquisition depend on cell size (Morel and Bricaud 1981, Reynolds 1984, Chisholm 1992), which therefore determines growth rates and the ability of a phytoplankter to compete with other cells for resources. Cell behavior, namely sinking and possibly swimming, is also a function of size (Smayda 1970, Kamykowski and McCollum 1986, Sommer 1988). At the community level, interactions between phytoplankton and grazers are influenced by cell size via size-selective grazing and the dependence of encounter-based processes on cell size (Kiørboe 1997). Last, the fate of phytoplankton is largely controlled by cell size because both aggregate formation and sinking rates are size-dependent (Kiørboe 1997). Phytoplankton span 4 orders of magnitude in size, ranging from cells smaller than a micrometer to large diatom chains that can reach several millimeters in length. Size composition of phytoplankton assemblages varies greatly in space and time, leading to significant changes in structure and function of aquatic systems.

The promise of size spectra as a synoptic measure of structure and function of planktonic communities has long been recognized (e.g., Chisholm 1992) and has been assessed in several studies (Cavender-Bares et al. 2001, Sabetta et al. 2005), but measurements of particle size distribution (PSD) in general, and phytoplankton size distribution in particular, have always been a challenge. The most commonly practiced laboratory-based measurements such as microscopy or electrical sensing zone particle counters (Coulter, Elzone, flow cytometry), require isolation of particles from the environment and often involve sample preparation (e.g., addition of fixatives) and storage that may alter particle size distribution (Menden-Deuer et al. 2001). Furthermore, laboratory-based size measurements do not provide real-time data and are limited in their spatial and temporal coverage. Recognizing the need for in situ measurements of particle size distribution, Olson et al. (2003) developed a submersible flow cytometer (FlowCytobot) that can be operated remotely. They successfully demonstrated its utility in documenting seasonal and event-scale changes in size distribution and abundances of pico- and nanophytoplankton (Olson et al. 2003).

Among the commercially available particle-sizers, however, very few instruments are capable of autonomous measurements

Acknowledgments

We thank W. Slade, L. Pritchard, I. Cetinic, and J. Loftin for assistance with laboratory measurements and data analysis. S. Grant and J. Ahn kindly provided us with their field data. This manuscript has greatly benefited from comments by D. Townsend and two anonymous reviewers. The study was supported by NASA grant NAG5-12393 to L.K.-B. and ONR grant N00014-04-1-0710 to E.B.

of size distributions of micron-sized particles in situ. One of them is the LISST-100 (Laser In Situ Scattering and Transmissometry; Sequoia Scientific, Inc.), which uses near forward light scattering measurements to obtain information on the size and concentration of suspended particles. The LISST-100 is capable of sampling at a higher rate (1 Hz) than other particle sizers and is highly versatile; it can be used in flow-through, profiling, or moored modes as well as on a laboratory bench. The size range obtained by the LISST-100 depends on the specific model (1.2 to 250 μm for model B used in this study). Two other currently available commercial instruments that permit real time (or near real-time) in situ measurements of particle size distribution are the FlowCAM (Fluid Imaging Technologies) and an in situ flow cytometer (CytoBuoy b.v., the Netherlands). Unlike the latter instruments, in the LISST-100, in situ measurements do not require pumping of the sample into the instrument; thus it preserves the in situ size distribution (e.g., does not disrupt aggregates). In addition, the LISST-100 samples a larger volume of water (~2.5 mL/s) compared to the volume sampled by an instrument that analyzes individual particles (e.g., <0.005 μL/s for the CytoBuoy; Dubelaar and Gerritzen, 2000).

Other than microscopy, none of the sizing methods directly measure particle dimensions; rather, another physical measurement—e.g., light scattering (LISST-100 and flow cytometers) or electrical impedance (Coulter, Elzone)—is inverted to obtain a property descriptive of size (e.g., cross-sectional area, volume). Such inversions require assumptions about the particle's shape. Most commercial instruments report size as the equivalent spherical diameter (ESD), which refers to the diameter of a sphere that would exhibit the same physical characteristics as those exhibited by the particles in the examined sample (Jennings and Parslow 1988). It is important to keep in mind that different physical measurements are sensitive to different attributes of the particle (for example, whereas near-forward light scattering is sensitive to the particle's cross-sectional area, electrical impedance is sensitive to the particle's volume), and thus ESDs reported by one instrument may not be identical to those reported by another instrument, particularly in the case of nonspherical particles (Jennings and Parslow 1988).

Principles of LISST-100 operation and data inversion—A detailed description of the principle of operation of the LISST-100 and its data inversion have been published (Agrawal and Pottsmith 2000). In short, a collimated beam of light (from a laser source with a wavelength $\lambda = 670$ nm) that is scattered by an assemblage of particles is collected on a receiving detector that is comprised of 32 concentric ring photodetectors. The radii of the rings increase logarithmically, corresponding to a logarithmic spacing of particle size. Each ring measures scattering over a subrange of angles, together covering scattering angles of 1 to 15 degrees in water for the LISST-100 B (Slade and Boss 2006). Scattering by particles largely depends on the physical characteristics of the particles, namely their size, shape, and composition (i.e., index of refraction) (e.g., van de Hulst 1981, Bohren and Huffman 1983, Kirk 1994).

At small near-forward angles, scattering is dominated by diffraction (e.g., van de Hulst 1981, Bohren and Huffman 1983), which is most sensitive to the particle's cross section. The angular distribution of the intensity of the scattered light is therefore primarily determined by the size of the particles and their shape. As viewed by the ring detectors, small particles place maximum energy on the outer rings, whereas large particles place the maximum on inner rings (Agrawal and Pottsmith 2000, Slade and Boss 2006).

Scattering intensities detected by the different rings are recorded and then used to solve a matrix equation that provides a volume concentration as function of ESD. The inversion algorithm is a modified Chahine method (Agrawal and Pottsmith, 2000). Inversion is performed using a kernel matrix that is based on Mie theory which provides the solution for the interactions of a plane parallel light with homogeneous spheres. Thus, a fundamental assumption of the LISST-100 inversion is that particles behave like homogeneous spheres or that they can be represented well by such a model. Because the LISST-100 was originally designed for sediment transport studies, the index of refraction used in the construction of the kernel matrix is that of inorganic-like particles (the real part of the index of refraction, $n = 1.15$, and the imaginary part is assumed to be 0). Organic-like particles, such as phytoplankton, have a real index of refraction closer to that of water itself, e.g., 1.05, due mostly to their high water content (Aas 1996), and also have a nonnegligible imaginary part at 670 nm. As mentioned above, however, in the diffraction limit scattering is weakly dependent on particle composition and hence the choice of index of refraction is not expected to alter significantly the inversion's results for phytoplankton. The analysis software corrects for attenuation along the path, and thus absorption effects associated with phytoplankton pigments are not expected to cause a significant deviation.

Applications of the LISST—Application of the LISST-100 series for laboratory and field studies has been extensively evaluated for sediments (Traykovski et al. 1999, Pedocchi and Garciá 2006), but its utility for biological applications has not been carefully assessed. An exception is a study by Serra et al. (2001) that demonstrates the utility of the LISST-100 in detecting and estimating concentrations of purple sulfur bacteria in lakes and measuring their vertical distributions (Serra et al. 2003a). The LISST-100 was also applied to study effects of turbulence on vertical and horizontal distributions of phytoplankton (Serra et al. 2003b). Peaks in the size spectra obtained by the LISST-100 were associated with different phytoplankton taxonomic groups based on characteristic cell dimensions from the literature and some measurements of cells dimensions using microscopy, but without validation of the size distributions and volume concentrations obtained by the LISST-100 (Serra et al. 2003b). Recently, the value of the LISST-100 in monitoring water quality, including harmful

algal bloom (HAB) events, has been demonstrated (Ahn and Grant 2007). Its general application for phytoplankton studies requires further evaluation, however, especially given the richness of cell shapes displayed by phytoplankton. For example, Ahn and Grant (2007) showed that during a dinoflagellate bloom there was good agreement between LISST-100 measurements of PSD and the PSD obtained by optical micrographs, but that was not the case for all bloom-impacted samples. Discrepancies between LISST-100 measurements and data from optical micrographs may have resulted from a failure of the LISST-100 to resolve phytoplankton of different sizes and shapes or because the image analysis software could not separate between cells in close proximity and counted them as a single particle (Ahn and Grant 2007); resolving this issue was out of the scope of their work.

In the diffraction limit (near-forward scattering), when particles are much larger than the wavelength of light, scattering is most sensitive to the cross-sectional area of the particle (e.g., van de Hulst 1981, Bohren and Huffman 1983). Inversions based on a model for spheres may provide poor estimates of the PSD of phytoplankton and other nonspherical particles for two main reasons (Jonasz 1987, Pedocchi and Garciá 2006; reviewed in Calvano et al. 2007): (1) a sphere is an extreme shape; of all convex shapes it has the smallest cross-sectional area–to-volume ratio; (2) for nonspherical particles, the cross-sectional area will depend on the orientation of the particle relative to the beam of light. Although the literature suggests that phytoplankton shape may significantly affect near-forward scattering patterns (MacCallum et al. 2004), a systematic evaluation of the effects of the cell shape (or the shape of any other natural particle) on LISST-100 inversions to obtain particle size is lacking. We report here the results of a laboratory study that examined the effects of cell shape on LISST-100 estimates of size and volume concentration, using phytoplankton cultures of varying cell sizes and shapes. We present results of a comparison between LISST-100 and microscopy measurements, discuss potential biases associated with the LISST-100 method, and provide examples for the use of the LISST-100 in laboratory and field studies of phytoplankton ecology.

Materials and methods

Phytoplankton cultures—Measurements were made with 8 species, including the dinoflagellates *Alexandrium tamarense* (CCMP115), *Gymnodinium simplex* (CCMP419), *Lingulodinium polyedra* (CCMP1931), and *Ceratium longipes* (CCMP1770) and the diatoms *Ditylum brightwellii* (CCMP2227) and *Coscinodiscus radiatus* (CCMP312), and 2 chain-forming species, *Stephanopyxis turris* (CCMP815) and *Skeletonema costatum* (CCMP784). These species were chosen because they are commonly found in coastal waters and encompass a wide range of cell (or chain) sizes and shapes. We also included HAB species; one of them, *L. polyedra*, is known to form nearly monospecific blooms. All cultures were grown in L1-enriched sterile seawater media (Guillard and Hargraves 1993). Cultures were maintained at 17°C with illumination of approximately 100 μmol photons $m^{-2}s^{-1}$ and a 14:10-h light-dark cycle. To minimize the effects of particles other than phytoplankton cells on the LISST-100 measurements, the following procedure was used for media preparation. Seawater collected from the Damariscotta estuary (Maine) was filtered through a 0.7-μm GF/F filter. Nutrients were added and the medium was sterilized. The cooled sterile medium was then sterile-filtered through a 0.2-μm filter (Steritop; Millipore) to remove any particles formed during sterilization.

LISST-100 measurements: data collection and data analysis—Measurements were conducted with a LISST-100, type B. Validation of its performance was done in an earlier study, using spherical beads of known size and refractive index (Slade and Boss 2005). For phytoplankton measurements, the LISST-100 was fitted with a small-volume, full-path chamber (purchased from the manufacturer). The chamber was filled with ~100 mL of a culture sample, and data were recorded using LISST-SOP software (averaging 100 instrumental samples obtained at 1 Hz). Although the chamber has a built-in magnetic stirrer, we chose to record scattering without using the stirrer to avoid potential cell damage. We found in preliminary experiments that over the short period of measurements (<2 min), settling did not significantly affect the results (data not shown). Measurements of background scattering were conducted before each phytoplankton measurement using deionized water (for comparison with manufacturer calibration) and 0.22 μm filtered sea water of the same source from which medium was prepared (used as blanks and subtracted from phytoplankton measurements). Data were processed and inverted to obtain cell size and volume concentration using MatLab programs (provided by Sequoia Scientific, Inc). Volume concentrations were converted to cell number concentrations (number of cells per milliliter) by dividing volume concentration at each size bin by the volume of a sphere of the same diameter as the median ESD of the bin.

Microscopy—Phytoplankton samples were taken from the LISST-100 chamber after each measurement and immediately preserved with buffered formalin (1% final concentration; see Discussion). Cell (or chain) numbers were counted under a Nikon Optiphot-2 microscope using a Sedgwick-Rafter cell (triplicate samples of 1 mL each), and the dimensions of 50 to 106 cells (or chains) were measured (Table 1). For all species, 2 linear dimensions were measured: (1) length, which was defined as the largest straight line between 2 points on the cell boundary that parallels the cell's axis of rotation, and (2) width, which was defined as the largest straight line between two points on the cell boundary that parallels the equatorial axis of the cell (i.e., at 90 degrees to length). The 3rd dimension (depth) was assumed to be equal to the minor axis, except when noted otherwise. These measurements were used in the calculations of cell (or chain) volumes, surface areas, and aspect ratios (the ratio between the major and minor axes of a cell or a chain). The aspect ratio is used here as an indicator of

Table 1. Cell (chain) size and concentration measured by microscopy and the LISST-100

Species	Aspect ratio	Microscopy ESD_c μm	Microscopy ESD_v μm	No. of measured cells (chains)	mode ESD LISST (bin range, μm)	Cell (chain) concentration, n/mL Microscopy	Cell (chain) concentration, n/mL LISST
G. simplex	1.1 ± 0.1	16.4	16	60	12.7–15	2825 ± 138	1438; 11 < ESD < 17
A. tamarense	1.1 ± 0.04	31.5	31.4	106	29–34.2	96	136; 26 < ESD < 38
L. polyedra	1.1 ± 0.1	43.2	43.2	100	40.4–47.7	241	124; 33 < ESD < 62
C. radiatus	0.85 ± 0.1	52	52	55	47.7–56.2	1002 ± 80	1107; 38 < ESD < 68
D. brightwellii	3.2 ± 1.4	37.3	26.8	100	29-34.2	514 ± 13	425; 24 < ESD < 67
S. turris	9.5 ± 5.1	85.4	61.3	100	3 modes: 29–34.2, 56.2–66.4, 78.3–92.4	19 ± 7	35; 39 < ESD < 155
S. costatum	10.8 ± 4.5	31.6	22.7	50	6.5–7.7	5270 ± 20	267[a]; 19 < ESD < 49
C. longipes	Core body 1 ± 0.2 Spine 8.7 ± 1.9	72.4	61.3	105	3 modes: 9.1–10.7, 47.7–56.2, 151.9–179.2	19 ± 1	10; 47 < ESD < 78

[a]4761; encompasses the range of minimum and maximum measured dimension (8–204 μm).

the deviation from a spherical shape, where the aspect ratio of a sphere equals 1.

For single cells of a relatively simple geometry (*A. tamarense*, *L. polyedra*, *G. simplex*), cell volume and surface area were calculated based on a model of a spheroid. For *Coscinodiscus radiatus*, cell volume and surface area were calculated using a model of a cylinder. Volumes and surface areas of the 2 chain-forming species (*S. turris*, *S. costatum*) were also calculated based on a model of a cylinder, using measurements of total chain length and chain width. Our choice of shape likely overestimates the volume of chains and underestimates the cross-sectional areas, since the gaps between cells in a chain are included in the calculations. For these 2 species, however, gaps between cells account for <10% of the total length of chains. The other approach to volume and surface area calculations, which is based on size measurements of selected cells and multiplying an average cell size by the number of cells in a chain, will result in an error of a similar order of magnitude due to variations in cell sizes within chains.

A geometric model suggested by Hillebran et al. (1999) was used to calculate volume and surface area of *D. brightwellii*. This model of a prism on a triangular base requires a 3rd dimension, which was calculated from width measurements in the apical plane (girdle view), assuming an equilateral triangular base. Cell volume and surface areas for *C. longipes* were also calculated according to Hillebran et al. (1999), using a model of a spheroid, a cylinder (apical spine), and 2 cones (antapical spines). Additional measurements included the length and width of the apical horn.

For each cell, measurements of surface area were then used to calculate an average cross-sectional area over all orientations (recall that the LISST-100 records data of an assembly of cells of presumably random orientation and that the cross-sectional area of a cell depends on its orientation relative to the beam of light). For any convex shape the average cross-sectional area over all orientations equals one quarter of its surface area (Cauchy 1832). Calculated volumes and cross-sectional areas were translated into a linear dimension (ESD). Two ESDs were computed for the comparison with LISST-100 data: (1) ESD_c, equivalent spherical diameter of a sphere of an equal cross-sectional area, was expected to show better fit to the LISST-100 data, as the optical measurement is most sensitive to the cross-sectional area of a particle and not to its volume; (2) ESD_v, equivalent spherical diameter of an equal volume sphere, is a quantity equivalent to that provided by a Coulter counter and is important for many biogeochemical studies that attempt to constrain biomass. For comparisons, computed ESDs were divided into 32 size bins that match the size bins of the LISST.

Measurements of temporal changes in cell size distribution in a culture of the diatom C. radiatus—As part of a study on sexual reproduction in *C. radiatus,* we monitored changes in cell size distributions in a semicontinuous batch culture, for a period of several months. The culture was grown in a L1-enriched sterile seawater media and maintained at 17°C with illumination of approximately 70 μmol photons $m^{-2}s^{-1}$ and a 14:10-h light-dark cycle. Samples for cell size measurements were taken weekly or biweekly. Cell sizes were determined from LISST-100 measurements (as described above) and microscopy. Microscopy samples were also used for identification of gametes and auxospores.

Results and discussion

Comparison of size distributions determined by LISST-100 and microscopy—For cells with a nearly spherical shape (aspect ratio not significantly different from 1; Table 1), there is a good agreement between the LISST-100 and microscopy with respect to the shape of the size distribution curve and its mode (Figure 1, Table 1). As aspect ratios of cells depart from unity (e.g., *C. radiatus*, *D. brightwellii*), LISST-based and microscopy-based size distributions deviate, with the LISST-100 showing a

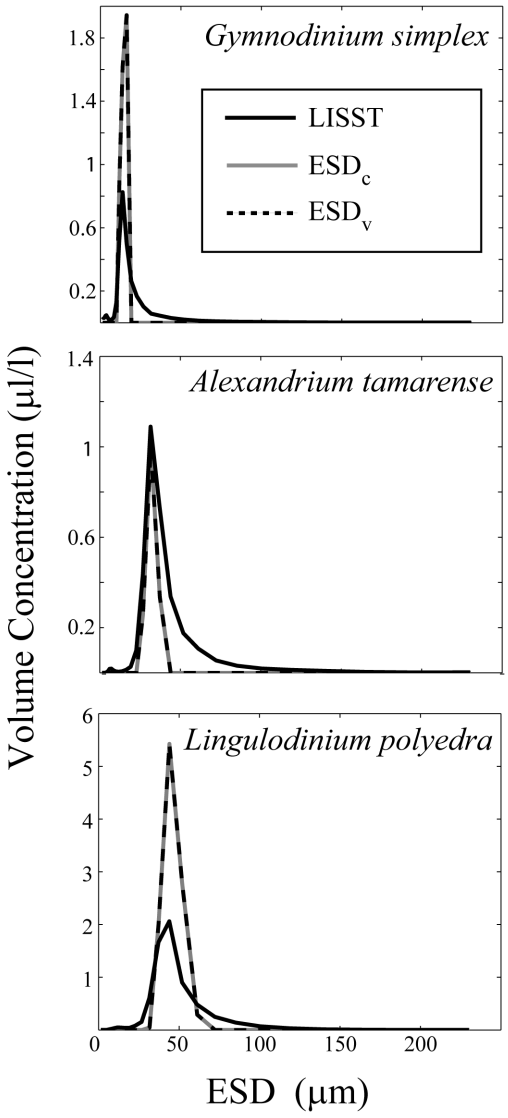

Fig. 1. Volume concentration (µL/L) as a function of ESD (µm) for 3 species of dinoflagellates with aspect ratios not significantly different from 1 (Table 1). LISST-100 data are represented by the black solid line. Microscopy data are represented by the gray line (ESD_c, equivalent spherical diameter of a sphere of an equal cross-sectional area) and the dashed black line (ESD_v, equivalent spherical diameter of an equal volume sphere).

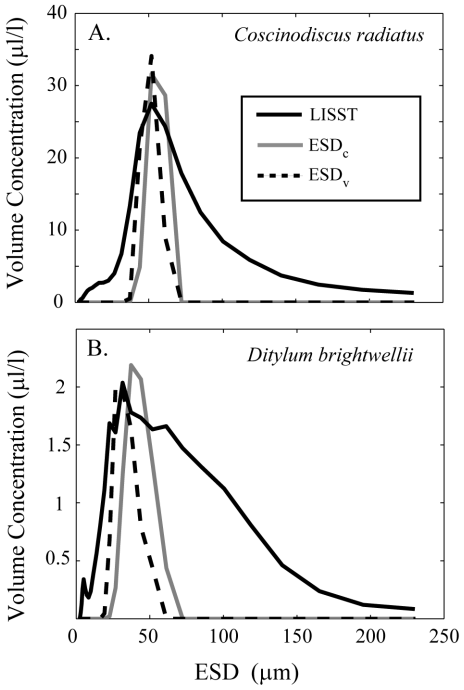

Fig. 2. As in Figure 1 except for 2 species of diatoms with aspect ratios larger than 1 (Table 1). LISST-100 data are represented by the black solid line. Microscopy data are represented by the gray line (ESD_c) and the dashed black line (ESD_v).

wider PSD than that obtained from microscopy (Figure 2). However, there still exists a good agreement between the modes obtained by the two methods (Table 1).

For species that deviate significantly from a spherical shape (e.g., *S. turris*, *S. costatum*, and *C. longipes*), the two methods show poor agreement. Size distributions obtained from LISST-100 measurements show a wider range compared with distributions obtained from microscopy and often exhibit multiple peaks (Figures 3 and 4). In contrast, PSDs based on microscopy typically show 1 distinct mode. Furthermore, the PSD based on cross-sectional area calculations (ESD_c) and the PSD based on cell volume calculations (ESD_v) are shifted with respect to their modes, with modes of cross-sectional-area–based PSD always corresponding to a larger equivalent spherical diameter than the modes of the volume-based PSD (Figures 3 and 4).

LISST-100 data for *S. costatum*, a chain-forming species, show a broad and fairly flat size distribution, with a peak at 7.1 µm (Figure 3A). This peak is likely associated with the width of the chains (mean chain width obtained from microscopy, 9.2 ± 1.2 µm). For *S. turris*, another chain-forming species, LISST-100 data are multimodal, with 3 distinct peaks (Figure 3B); 2 of the peaks match the modes calculated by microscopy for ESD_c and ESD_v (Figure 3B, Table 1).

LISST-100 data for *C. longipes* also show 3 peaks (Figure 4); each appears to be associated with a different size characteristic of the cell. The highest peak is broad and encompasses sizes (ESDs) ranging between 140 and 164 µm. It is associated with the ESD of an imaginary spheroid that encompasses the entire ventral view (cross-sectional area) of the cell, including its spines (Figure 4), with mean ESD_c and ESD_v of 152 and 156 µm, respectively. A 2nd peak (ESD 51.9 µm) is associated with the body of the cell (without its spines, Figure 4; ESD_c and ESD_v calculations from measurements of the body itself are 54 and 59, respectively). The 3rd, smallest peak has an ESD of 9.9 µm and appears to be associated with the width of a spine (mean width of spine, 11.3 ± 1.4 µm).

Several factors may contribute to the differences observed between size spectra obtained by the LISST-100 and those obtained from microscopy measurements. (1) The LISST-100

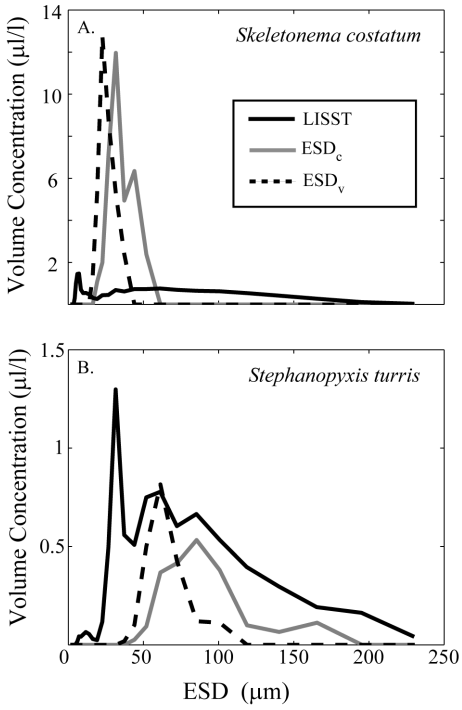

Fig. 3. Volume concentration (µL/L) as a function of ESD (µm) for 2 chain-forming diatoms with aspect ratios that are significantly larger than 1 (Table 1). LISST-100 data are represented by the black solid line. Microscopy data are represented by the gray line (ESD_c) and the dashed black line (ESD_v). The 2nd small peak in the ESD_c curve (top panel) is not significant and is due to an artifact associated with the binning procedure and the small sample size of chains that were measured (n = 50).

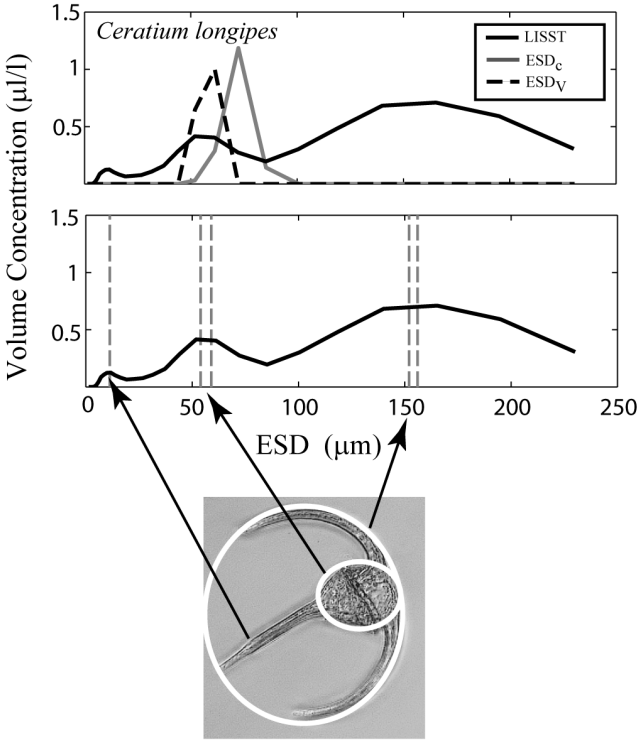

Fig. 4. Top panel: volume concentration (µL/L) as a function of ESD (µm) for *C. longipes*. LISST data are represented by the black solid line. Microscopy data are represented by the gray line (ESD_c) and the dashed black line (ESD_v). Bottom panel: the same LISST data as in top panel (solid black line). Vertical dashed lines represent mean values of ESD_c and ESD_v calculated from microscopy for (1) the imaginary spheroid that encompasses the entire ventral view (cross-sectional area) of the cell (including its spines), (2) the body of the cell (without its spines), and (3) the mean width of a spine. Arrows drawn from an image of the cell refer to the ESDs associated with these 3 cell dimensions.

measures near-forward scattering, which is most sensitive to the cross-sectional areas of cells perpendicular to the beam of light. A culture of nonspherical cells will display a polydispersion of cross sections due to the different orientations presented to the beam. Indeed, Paramonov (1994) has shown that the absorption and scattering coefficients of a suspension of a monodispersion of identical spheroids can be modeled by a polydispersion of spheres with the same index of refraction. With microscopy, however, the same cross-sectional area is typically observed for all cells (as cells tend to lay flat on the microscope slide), and the average cross-sectional area is obtained from theoretical calculations [using Cauchy's (1832) rule]. (2) PSDs obtained from microscopy measurements are based on simplifying assumptions regarding the shape of cells and chains with a sample size that is at least an order of magnitude smaller than that sampled by the LISST. (3) Microscopy measurements were conducted on preserved cells. Preservation can result in cell shrinkage or swelling, depending on the species (Booth 1987, Menden Deuer et al. 2001). Quantification of the effect of preservation on cell size (volume) of diatoms and dinoflagellates has been reported for fixatives such as Lugol and glutaraldehyde, revealing variations between fixed and nonfixed samples of up to 60% (Menden Deuer et al., 2001); we are not aware of a similar study for formalin. (4) The sample always contains particles other than the cells, which are detected by the LISST-100 but not included in the microscopy analysis. Although extreme care was taken to minimize the effect of nonliving particles on the measurements (i.e., prefiltration of media thorough 0.2-µm filter, maintenance of cells in exponential phase), the presence of such particles in the media is unavoidable.

To examine the potential contamination of LISST-100 results by other particles, we repeated the measurements for cultures of *C. radiatus* and *C. longipes.* Cultures were then filtered through a 53-µm Nitex mesh (just below the mode of *C. radiatus*, and within the mode of *C. longipes*; Figure 5), and the filtrate was placed back in the LISST-100 chamber for an additional measurement. The LISST-100 chamber was carefully rinsed with filtered seawater (0.22 µm) between culture and filtrate measurements. If particles smaller than 53 µm contributed significantly to the signal observed for size bins with ESD <53 µm, we would expect this signal to remain after the filtration. The LISST-100 signal in this size range (2 < ESD < 53), however, decreased dramatically after the removal of

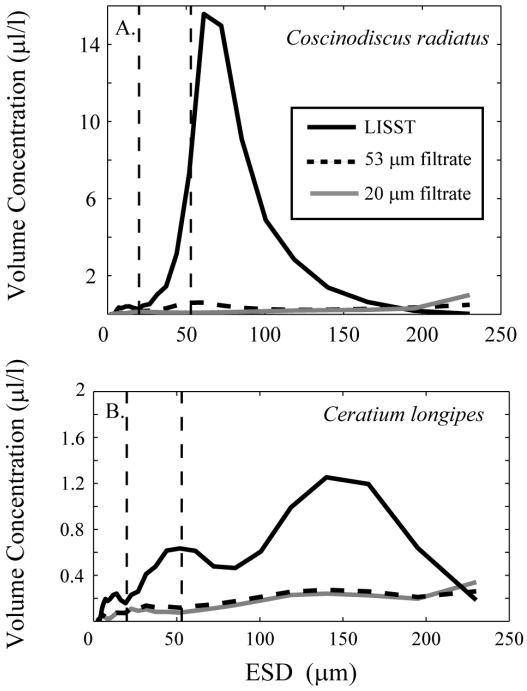

Fig. 5. A comparison between LISST-100 measurements of size distribution of cells in a culture (solid black line) and filtrates of the same culture using a 53-μm Nitex mesh (dashed black line) and a 20-μm Nitex mesh (solid gray line) for *C. radiatus* (A) and *C. longipes* (B). Vertical dashed lines represent the size cutoff for each of the filtrations.

cells (Figure 5), indicating that the size distribution measured for the culture (at least within this size range) was primarily associated with cells and their different orientations rather than with other particles. The filtrate was further filtered through a 20-μm Nitex mesh to examine if the smaller mode observed in the case of *C. longipes* is indeed associated with the spines of the cells or with other small particles suspended in the medium. Again, results indicate that this mode was associated with the whole cells and not with other small (<20 μm) particles in the medium (Figure 5B).

Given the fundamental differences between the two sizing methods used here, the similarities observed for the particle size distribution modes for species of relatively simple shapes are striking, demonstrating the utility of the LISST-100 in sizing cells that are nearly spherical in shape, or cylindrical, with an aspect ratio not much different from 1 (e.g., *C. radiatus*, *D. brightwellii*). Furthermore, when only the size bins that encompass the range of ESDs calculated from microscopy are accounted for, estimates of cell concentrations obtained from the LISST-100 are of the same order of magnitude as those obtained from microscopy (within 50% difference), except for *S. costatum* (Table 1). The good agreement between LISST-100 inversions and microscopy, despite differences between the index of refraction assumed by the inversion and that for phytoplankton, is testimony to the relative lack of sensitivity of near-forward scattering by such particles to their composition.

Size determination of nonspherical particles is often ambiguous, and the lack of better agreement between the LISST-100 and microscopy is not surprising. ESD is the most commonly used parameter to describe size of nonspherical particles, but it provides no information about shape; to describe shape, at least 1 additional parameter (e.g., aspect ratio for a spheroid) is needed. Moreover, the dependence of ESD on the major dimension and aspect ratio differs with the physical basis of the measurement (e.g., volume, cross-sectional area, sedimentation rate) and therefore one cannot expect different methods to yield similar results (Jennings and Parslow, 1988). This attribute is clearly seen in our microscopy data for *D. brightwellii*, *S. turris*, and *C. longipes* (Figure 4 and 5) where, for the same population of cells that were sized, ESD calculations based on cell volume do not coincide with ESD calculations based on cross-sectional area. The physical basis of the LISST-100 measurement (near-forward scattering) is closely linked with the particle's cross-sectional area. Based on theory, we expected ESD_c to show better fit to the LISST-100 data than ESD_v. This is not evident in our data, particularly for the species that form chains or have spines. One possible explanation is that the formulation for an average cross-sectional area of a randomly oriented particle (Cauchy 1832), which was applied in this study, is valid only for convex shapes. Forms that possess spines or chains that have gaps between cells or that are curved are not convex.

In this study, LISST-100 performance was compared to only 1 method of sizing. In an earlier study, profiles of particle concentrations obtained by LISST-100 and flow cytometry showed good agreement (Serra et al. 2001). This is not surprising, given that both methods rely on a measurement of near-forward light scattering. Other automated size analyzers, such as the Coulter counter, are sensitive to the particle's volume, and we would not expected results obtained by such analyzers to be identical to the LISST, particularly when nonspherical cells dominate the sample. These 2 methods, however, if done in concert, can be used to obtain information on the degree of nonsphericity of particles in the water (Jonasz 1987, Jennings and Parslow 1988).

Use of the LISST-100 in laboratory and field studies—An attractive feature of the LISST-100 is its high versatility; it can be used in the laboratory, on a boat, or on a mooring. Its relatively small footprint (13.3 cm in diameter by 81 cm in length) and light weight (12 kg in air) make it easy to use in all three applications. The laboratory measurements described above demonstrate the utility of the LISST-100 in measuring size and volume concentrations of cells with an aspect ratio that is close to 1. In this section, we provide examples for possible uses of the LISST-100 in laboratory and field studies.

Monitoring size changes in the laboratory is valuable for many studies concerning the ecology and physiology of phytoplankton. These include species competition and succession, phytoplankton-herbivore interactions (e.g., selective grazing), life cycles, and studies on physiological processes

that are often linked to cell size (e.g., growth rate). Two important groups of phytoplankton that undergo significant size transitions as part of their life cycles are diatoms and the prymnesiophyte, *Phaeocystis*. In diatoms, cell size and sexual reproduction are intimately linked. Vegetative cell division results in a progressive reduction of the mean cell size of a population (Round et al. 1990). Once a cell reaches a critical (cardinal) size, it must enlarge or it will die. The onset of sexual reproduction is the most common mechanism to restore cell size, although asexual cell enlargement also exists in some species (Chepurnov et al., 2004). Sexual stages are often difficult to detect, especially in the field. Inference of sexual reproduction often comes from measurements of cell size spectra, where the presence of large cells provides indirect evidence of sexual events (Mann 1988; Jewson 1992a, 1992b), but monitoring size changes using microscopy is laborious. Our laboratory experiments with a culture of *C. radiatus* clearly show that the LISST-100 was able to detect changes in mean cell size as the culture transitioned from an asexual to a sexual phase and that LISST-100 estimates of mean cell size (as indicated by the modes of the size distribution) followed closely those obtained by microscopy (Figure 6; for details, see caption). Microscopy will always be required for verification and identification of different life history stages, but the LISST-100 can reduce the labor associated with microscopy. It provides a rapid, nonintrusive method that can be used for both marine and freshwater phytoplankton. Other automated methods such as flow cytometry and Coulter counters have been successfully used in studies of the life cycle of marine diatoms (Armbrust and Chisholm 1992, von Dassow et al. 2006), but the LISST-100 offers several advantages over these methods. First, the LISST-100 does not require pumping or manipulation of a sample. This is particularly important when delicate life stages, such as auxospores, are considered. Furthermore, much of what we know about the sexual life of diatoms comes from studies on freshwater species (reviewed in Chepurnov et al. 2004). Coulter counters require that a sample of freshwater diatoms will be first mixed in a weak electrolyte solution; this may alter size through osmotic stresses (auxospores, for example, would be particularly sensitive to that). LISST-100 measurements, on the other hand, can be conducted with both marine and fresh water diatoms, without the need to manipulate samples. Second, at any given time, the volume that is sampled by the LISST-100 is much larger than that sampled by a flow cytometer or a Coulter counter (approximately 2.5 mL/s operating at 1 Hz). Last, the LISST-100 allows sizing of intermediate-size and large cells that traditionally have been more difficult to measure with a flow cytometer. Coulter counters allow sampling of a much wider size range (0.4 to 1200 μm) if several apertures are available, but each change of the aperture requires a new calibration. To obtain a full size spectrum of a culture, when several life stages of different cell sizes are simultaneously present (e.g., sexual and asexual cells in diatoms, solitary cells, and

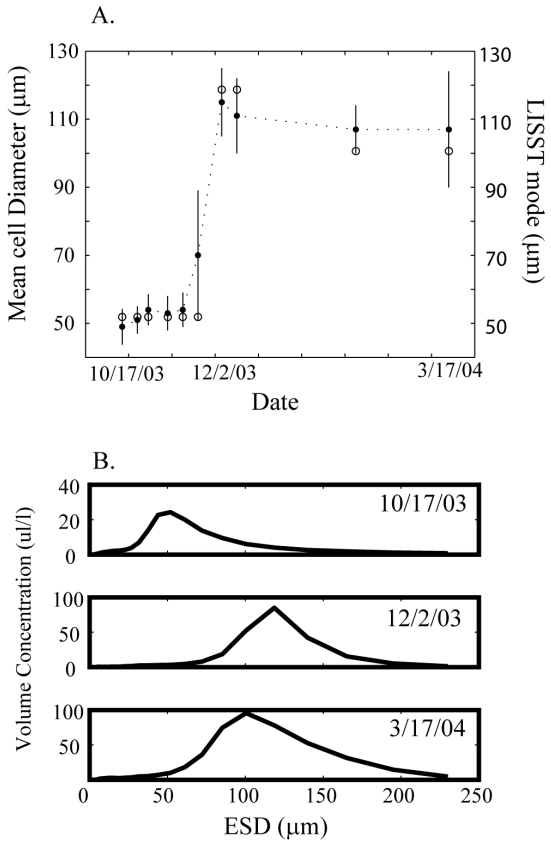

Fig. 6. (A) A time series of cell size in a semicontinuous batch culture of *C. radiatus.* Size based on microscopy (filled circles) is given here as mean cell diameter (with error bars spanning ± 1 SD) because we could not calculate ESDs in all samples; after sexual reproduction occurred, the large cells were situated such that we could only observe them in a valve view, thus we could not obtain their 2nd dimension. LISST data are presented as the mode of the size distribution in each sampling date (open circles). (B) LISST-100 size spectra for 3 dates. Note the shift in the modes as the culture of vegetative cells (top panel) went through a sexual phase (on 12/2/03; middle panel) and then began to divide asexually again (bottom panel).

colonies of *Phaeocystis*), will require multiple measurements when using a Coulter counter. The same limitation will apply to other laboratory experiments (e.g., competition, selective grazing) in which cultures contain a mixture of cells of a wide range of sizes. The LISST, although capable of measuring a smaller size range (1.2 to 250 μm for type B) than a Coulter counter, is able to provide that spectrum in one measurement. Although the LISST-B cannot define well the size of picoplankton, nor large colonies of *Phaecystis*, its size range is compatible with the size range of the majority of single-celled diatoms and dinoflagellates as well as solitary cells and small colonies of *Phaeocystis*.

Thus far, we have discussed the use of the LISST-100 with single-species cultures, but oceans and lakes are complex mixtures of phytoplankton and other organic and inorganic particles of varying sizes, shapes, and indices of refraction. Although the LISST-100 measures scattering at 32 angles,

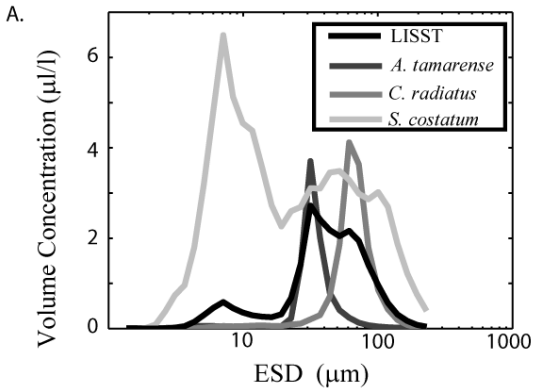

Figure 7. Size spectra of a mixture of cultures obtained by the LISST-100 (solid black line). Size spectra of each of the single-species cultures comprising the mixture are denoted in the background by the different gray lines (see insert in figure). Note that these measurements were conducted at a different time than the measurements reported in Figure 3. Differences in the size distribution of *S. costatum* between this figure and Figure 3 are likely due to changes in chain length distribution in the culture.

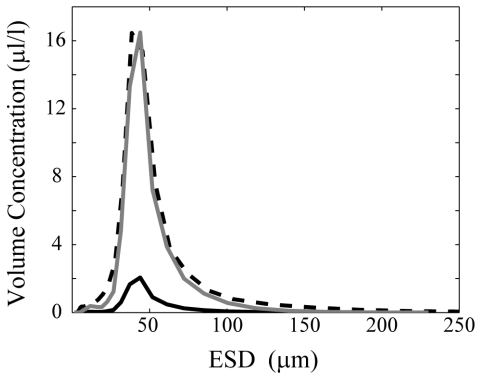

Fig. 8. A comparison of LISST data from field measurements during a bloom of *L. polyedra* (dashed black line; data were kindly provided by Ahn and Grant, University of California, Irvine, and published in Ahn and Grant 2007) and laboratory measurement of a culture of *L. polyedra* (CCMP1931; solid black line). For an easier comparison of the shape of the size distribution the culture concentration was scaled up (8×) to match the concentration of cells observed in the field (represented by the gray line). Note that concentrations used in our measurements are not exceptionally high and thus are relevant to field populations.

which theoretically correspond to 32 class sizes, in reality noise associated with the measurements and assumptions in the inversion reduce the size classes that can be resolved to about 10 to 12 (Agrawal, Sequoia Scientific, application note L008, www.sequoiasci.com). The capability of the LISST-100 to identify species or genus in a field sample depends on the relative size and concentration of the species (or genus) of interest with respect to the rest of the particles in the sample. LISST-100 measurements of mixtures of different species indicate that peaks associated with a specific species can be identified (Figure 7), as long as there exist sufficient size differences and as long as cells are not so diluted that their signature is masked. Laboratory characterization of LISST signatures of target species can aid in the interpretation of field data.

Our laboratory study suggests that during blooms characterized by high species diversity, such as diatom blooms (especially those of chain-forming species), LISST-100 data may be difficult to interpret. However, the LISST-100 can be a useful tool for monitoring monospecific or nearly monospecific blooms. There have been many cases reported of monospecific blooms. For instance, dinoflagellate blooms, in general, tend to have low species diversity and are often dominated by a single species (Smayda 1997, 2002). Examples include blooms of HAB species such as *Karenia breve* and *L. polyedra* in coastal waters and blooms of the genus *Peridinium* in lakes (Horne et al. 1971, Pollingher 1986). Nearly monospecific blooms have been also documented for other taxonomic groups including diatoms (Crawford 1995), brown tide algae (Bricelj and Lonsdale 1997), and prysemnophytes (Lancelot et al. 1998).

Conclusions from our laboratory measurements are supported by results from a recent field study in which seasonal variations in size distribution of particles were monitored in coastal water off Orange County, California, USA, using the LISST-100 and microscopy image analysis (Ahn and Grant 2007). Red tides are common in this coastal region. During near-shore blooms of *L. polyedra*, LISST-100 measurements of size distribution and volume concentrations were consistent with those obtained by image analysis (Ahn and Grant 2007). When comparing Ahn and Grant's (2007) field data to the measurements obtained in the laboratory for a culture of *L. polyedra*, the distributions are similar (Figure 8).

These results highlight the potential of the LISST-100 in monitoring programs, particularly in cases where target species are known and their LISST-100 size distribution signatures have been characterized. It provides a mean for real time, high-resolution (in space and time) measurements, and it can be used on moorings or deployed from a wide array of vessels (ranging from canoes to large research vessels) or from docks. Real-time monitoring is particularly important in the case of HABs, as it can provide an early warning system. It is important to reemphasize, however, that given the LISST-100 limitations associated with cell shape and its inability to distinguish between phytoplankton and other particles, complete understanding of phytoplankton (and more generally particle) dynamics will require auxiliary measurements in addition to the LISST, capable of providing bulk composition information (e.g., chlorophyll fluorescence or absorption and backscattering ratio; e.g., Boss et al. 2004), Microscopic examination of water samples will always be needed for validation of measurements, but the use of the LISST-100 can reduce the labor associated with microscopy. Also, as illustrated here, signatures of phytoplankton may not be unique, in particular for chain-forming species (e.g., compare *S. costatum* in Figure 3A and 7A, although in both cases a peak exists at 7.1 µm) and for species having different life stages (e.g., Figure 6). Furthermore, LISST-100 (type B) measurements are limited to size range of 2 to 250 µm, and hence are applicable to nano- and

microphytoplankton, but not to picoplankton. When dynamics of the entire phytoplankton community are of interest, LISST-100 measurements must be conducted together with flow cytometry measurements to encompass the full size spectrum of phytoplankton.

References

Aas, E. 1996. Refractive index of phytoplankton derived from its metabolite composition. J. Plankton Res. 18:2223–2249.

Ahn, J. H., and S. B. Grant. 2007. Size distributions, sources and seasonality of suspended particles in southern California marine bathing waters. Environ. Sci. Technol. 41:695-702.

Agrawal, Y. C., and H. C. Pottsmith. 2000. Instruments for particle size and settling velocity observations in sediment transport. Mar. Geol. 168:89-114.

Armbrust, E. V., and S. W. Chisholm. Patterns of cell size change in a marine centric diatom: variability evolving from clonal isolates. J. Phycol. 28:146-156.

Bohren, C. F., and D. R. Huffman. 1983. Absorption and Scattering of Light by Small Particles. New York: Wiley.

Booth, B. C. 1987. The use of autofluorescence for analyzing oceanic phytoplankton communities. Bot. Mar. 30:101–108.

Boss E., W. S. Pegau, M. Lee, M. S. Twardowski, E. Shybanov, G. Korotaev, and F. Baratange, 2004. Particulate backscattering ratio at LEO 15 and its use to study particles composition and distribution. J. Geophys. Res., 109, C1, C0101410.1029/2002JC001514.

Bricelj, V. M., and D. J. Lonsdale. 1997. *Aureococcus anophagefferens*: causes and ecological consequences of brown tides in U.S. mid-Atlantic coastal waters. Limno. Oceanogr. 42:1023–1038.

Calvano, W. R., E. Boss, and L. Karp-Boss. 2007. Inherent optical properties of non-spherical marine-like particles: from theory to observation. Oceanogr. Mar. Biol. Annu. Rev. 1-38.

Cauchy, A. L. 1832. Mémoire sur la rectification des courbes et la quadrature des surfaces courbes. France: Académie des Sciences.

Cavender-Bares K. S., A. Rinaldo, and S. W. Chisholm 2001. Microbial size spectra from natural and nutrient enriched ecosystems. Limnol. Oceanogr. 46:778-789.

Chepurnov, V. A., D. G. Mann, K. Sabbe, and W. Vyverman. 2004. Experimental studies on sexual reproduction in diatoms. Int. Rev. Cytol. 237:91-154.

Chisholm, S. W. 1992. Phytoplankton size. *In* P. G. Falkowski and A. D. Woodhead (eds), Primary Productivity and Biogeochemical Cycles in the Sea. New York, Plenum Press, p. 213-237.

Crawford, R. M. 1995. The role of sex in the sedimentation of a marine diatom bloom. Limnol. Oceanogr. 40:200-204.

Dubelaar, G. B. J., and P. L. Gerritzen. 2000. CytoBuoy: a step forward towards using flow cytometry in operational oceanography. Sci. Marina. 64:255-265.

Guillard, R. R. L., and P. E. Hargraves. 1993. *Stichochrysis immobilis* is a diatom, not a chrysophyte. Phycologia 32:234-236.

Hillebran, H., C. D. Dürselen, D. Kirschtel, U. Pollingher, and T. Zohari. 1999. Biovolume calculation for pelagic and benthic microalgae. J. Phycol. 35:403-424.

Horne, A. J., P. Javornicky, and C. R. Goldman. 1971. A freshwater red tide on Clear Lake, California. Limnol. Oceanogr. 16:684.689.

Jennings, B. R., and K. Parslow. 1988. Particle size measurement: the equivalent spherical diameter. Proc. R. Soc. Lond. 419:137-149.

Jewson, D. H. 1992a. Size reduction, reproductive strategy and the life cycle of a centric diatom. Phil. Trans. R. Sot. Lond. Ser. B 335:191-213.

———. 1992b. Life cycle of a *Stephanodiscus* sp. (Bacillariophyta). J. Phycol. 28:856-866.

Jonasz, M. 1987. Nonsphericity of suspended marine particles and its influence on light scattering. Limnol. Oceanogr. 32: 1059-1065.

Kamykowski, D., and S. A. McCollum. 1986. The temperature acclimatized swimming speed of selected marine dinoflagellates. J. Plankton Res. 8:275-287.

Kiørboe, T. 1997. Small-scale turbulence, marine snow formation and planktivorous feeding. Sci. Marina. 61:141-158.

Kirk, J. T. O. 1994, Light and Photosynthesis in Aquatic Ecosystems. Cambridge: Cambridge University Press.

Lancelot, C., G, Billen, A. Sournia, T. Weisse., F. Colijn, M. J. W. Veldhuis, A. Davies, and P. Wassmann. 1987. Phaeocystis blooms and nutrient enrichment in the continental coastal zones of the North Sea. Ambio 16:38–46.

Lancelot, C., M. D. Keller, V. Rousseau, W. O. Smith Jr., S. Mathot. 1998. Autecology of the marine haptophyte Phaeocystis sp., p. 209–224. *In* D. M. Anderson, A. D. Cembella, and G. M. Hallegraeff [eds]. Physiological ecology of harmful blooms. NATO ASI Series G, vol. 41. Springer.

MacCallum I., A. Cunningham, and D. McKee. 2004. The measurement and modeling of light scattering by phytoplankton cells at narrow forward angles. Opt. A: Pure Appl. Opt. 6:698-702.

Mann, D.G. 1988. Why didn't Lund see sex in *Asterionella*? A discussion of the diatom life cycle in nature. *In* F.E. Round (ed.), Algae and the Aquatic Environment. Bristol, Biopress, p. 383-412.

Menden-Deuer, S., A. J. Lessard, and S. Satterberg. 2001. Effect of preservation on dinoflagellates and diatom cell volume and cosequences for carbon biomass predictions. Mar. Ecol. Prog. Ser. 222:41-50.

Morel, A., and A. Bricaud. 1981. Theoretical results concerning light absorption in a discrete medium and application to specific absorption of phytoplankton. Deep-Sea Res. 28: 1375-1393.

Olson, R. J., A. Shalapyonok, and H. M. Sosik. 2003. An automated submersible flow cytometer for analyzing pico and nanophytoplankton: FlowCytobot. Deep-Sea Res. I 50: 301–15.

Paramonov, L. E. 1994. On optical equivalence of randomly

oriented ellipsoidal and polydisperse spherical particles: the extinction, scattering and absorption cross sections. Optics Spectrosc. 77: 589–592. [translated from Optika i Spektroskopiya]

Pedocchi F., and M. H. Garciá. 2006. Evaluation of the LISST-ST instrument for suspended particle size distribution and settling velocity measurements. Continental Shelf Res. 26: 943–958.

Pollingher, U. 1986. Phytoplankton periodicity in a subtropical lake (Lake Kinneret, Israel). Hydrobiologia 138: 127-138.

Reynolds, C. S. 1984. The Ecology of Freshwater Phytoplankton. Cambridge, Cambridge University Press.

Round, F. E., R. M. Crawford, and Mann, D. G. 1990. The Diatoms: Biology and Morphology of the Genera. Cambridge, Cambridge University Press.

Sabetta L., A. Fiocca, L. Margheriti, F. Vignes, A. Basset, O. Mangoni, G. C. Carrada, N. Ruggieri, and C. Ianni. 2005. Body size-abundance distributions of nano- and microphytoplankton guilds in coastal marine ecosystems. Estuarine Coastal Shelf Sci. 63:645-663.

Serra, T., J. Colomer, X. P. Cristina, X. Vila, J. B. Arellano, and X. Casamitjana. 2001. Evaluation of laser in-situ scattering instrument for measuring the concentration of phytoplankton, purpule sulfur bacteria, and suspended inorganic sediments in lakes. J. Envir. Eng. Nov.:1023-1030

———, L. Colomer, M. Soler, and X. Vila. 2003a. Spatio-temporal heterogeneity in planktonic thiocystis minor population, studied by laser in situ particle analysis. Freshwater Biol. 48:698-708.

———, T. Granata, J. Colomer, A. Stips, F. Mohlenberg, and X. Casamitjana. 2003b. The role of advection and turbulent mixing in the vertical distribution of phytoplankton. Estuarine Coastal Shelf Sci. 56:53-62.

Slade, W. H., and E. Boss. 2006. Calibrated near-forward volume scattering function obtained from the LISST particle size. Optics Express 14:3602-3615.

Smayda, T. J. 1970. The suspension and sinking of phytoplankton in the sea. Oceanogr. Mar. Biol. Annu. Rev. 8: 353-414.

———. 1997. Harmful algal blooms: their ecophysiology and general relevance to phytoplankton blooms in the sea. Limnol. Oceanogr. 42:1137–1153.

———. 2002. Adaptive ecology, growth strategies and the global bloom expansion of dinoflagellates. J. Oceanog. 58: 281-294.

Sommer, U. 1988. Some size relationships in phytoflagellate motility. Hydrobiologia 161:125-131.

Traykovski P., R. Latter, and J. D. Irish. 1999. A laboratory evaluation of the LISST instrument using natural sediments. Mar. Geol. 159:355-367.

van de Hulst, H.C. 1981. Light scattering by small particles. New York: Dover.

von Dassow, P., V. Chepurnov, E. V. Armbrust. 2006. Relationships between growth rate, cell size, and induction of spermatogenesis in the centric diatom *Thalassiosira weissflogii* (Bacillariophyta). J. Phycol. 42:887-899.

Submitted 23 March 2007
Revised 16 August 2007
Accepted 10 September 2007